Available online at www.sciencedirect.com
SCIENCE DIRECT®
Journal of Solid State Chemistry 177 (2004) 3346–3350
JOURNAL OF SOLID STATE CHEMISTRY
http://elsevier.com/locate/jssc

Hydrothermal synthesis of Nd^{3+}-doped orthoborate nanoparticles that emit in the near-infrared

Feng Wang,[a] Xianping Fan,[a,b,*] Daibo Pi,[a] and Minquan Wang[a,b]

[a] *Department of Materials Science and Engineering, Institute of Inorganic Materials, Zhejiang University, Zheda Road, Number 38, Hangzhou city, Zhejiang province, Hangzhou 310027, PR China*

[b] *State Key Laboratory of Silicon Materials, Zhejiang University, Hangzhou 310027, PR China*

Received 6 April 2004; received in revised form 20 May 2004; accepted 22 May 2004

Available online 20 July 2004

Abstract

The $Y_{1-x}BO_3:Nd_x$ nanoparticles have been prepared by a mild hydrothermal method and luminescence properties in the NIR of $Y_{1-x}BO_3:Nd_x$ nanoparticles have been investigated. The $Y_{1-x}BO_3:Nd_x$ nanoparticles with 0–15 mol% Nd^{3+} were found to be isostructural with YBO_3 crystal. The preferential nucleation and growth of $Y_{1-x}BO_3:Nd_x$ nanoparticles along a certain plane can be observed and the dopants of Nd^{3+} ions would help to weaken the selectivity of the growth of $Y_{1-x}BO_3:Nd_x$ nanoparticles. The emission spectrum in the NIR of $Y_{1-x}BO_3:Nd_x$ nanoparticles consisted of a few narrow, sharp lines corresponding to the $^4F_{3/2}\rightarrow{}^4I_{11/2}$ and $^4F_{3/2}\rightarrow{}^4I_{13/2}$ transitions of Nd^{3+} ions when pumped with 800 nm laser radiation. The luminescence intensity of $Y_{1-x}BO_3:Nd_x$ nanoparticles increased remarkably with the increase in the doping concentration of Nd^{3+} ions and reached a maximum at approximately 10 mol%.

Keywords: Hydrothermal; Nanoparticles; Nd^{3+} ions; Luminescence in the NIR

1. Introduction

During the past few years, the synthesis process and spectroscopic properties of the lanthanide-doped nanoparticles have attracted considerable interest since they are considered as potentially useful active components in lamps and displays [1], lasers [2], and new optoelectronic devices [3,4], etc. Various synthesis techniques of the lanthanide-doped nanoparticles and their luminescence properties have been reported previously [5–8].

Yttrium and lanthanide orthoborates have high UV transparency and exceptional optical damage threshold, which make them attractive for numerous practical applications. For example, the (Y, Gd)$BO_3:Eu^{3+}$ phosphors were extensively used as red phosphors for display [9] and have been adequately investigated. The conventional process of preparing (Y, Gd)BO_3 phosphors such as solid-state reaction [10,11] and flux-aided solid-state reaction [12] involves a high temperature of above 1000°C and a milling step, leading to a poor crystalline integrity [11] and damaged luminescent properties [13]. Therefore, many efforts had been made to find novel low temperature synthetic procedures. Wang et al. synthesized successfully non-aggregated $GdBO_3:Eu^{3+}$ particles by a mild hydrothermal method [14]. But only submicron-sized particles could be produced, since a relative high temperature (300°C) was needed. Recently, Jiang et al. have prepared $YBO_3:Eu^{3+}$ nanoparticles by choosing the method of hydrothermal homogeneous urea precipitation [15]. In this two-step hydrothermal method, high-quality nanosized $YBO_3:Eu^{3+}$ particles could be synthesized at very low temperature (200°C).

The lanthanide(III)-doped nanoparticles that emit in the near-infrared region (NIR) would be of particular interest as active material in telecommunication components, lasers, and polymer displays, etc. Especially when used as fluorescent label in bioassays, high

*Corresponding author. Department of Materials Science and Engineering, Institute of Inorganic Materials, Zhejiang University, Zheda Road, Number 38, Hangzhou city, Zhejiang province, Hangzhou 310027, PR China. Fax: +86-571-8795-1234.

E-mail address: fanxp@cmsce.zju.edu.cn (X. Fan).

0022-4596/$ - see front matter © 2004 Elsevier Inc. All rights reserved.
doi:10.1016/j.jssc.2004.05.049

sensitivity of detection could be achieved due to the absence of interfering with background fluorescence by using luminescence in the NIR. To the best of our knowledge, only a few research works on the synthesis process and luminescence properties of the lanthanide(III)-doped nanoparticles that emit in the NIR have been reported. The synthesis process of the lanthanide(III)-doped yttrium orthoborates (YBO_3) that emit in the near-infrared has not been still investigated. Well-crystallized YBO_3 nanoparticles can be conveniently synthesized and higher concentration of lanthanide ions can be doped by the two-step hydrothermal method [15]. In this work, the synthesis process of $Y_{1-x}BO_3$:Nd_x nanoparticles by the hydrothermal method and their spectroscopic properties in the NIR have been described.

2. Experimental

$Y_{1-x}BO_3$:Nd_x nanoparticles were prepared according to a literature procedure [15]. The boric acid (0.04 mol/L), urea (0.05 mol/L), $YNO_3 \cdot 6H_2O$ and Nd_2O_3 were dissolved in dilute HNO_3, with the total concentration of metal cation being 0.04 mol/L and the initial pH value being 4. With doping concentration ranging from 0.025 to 0.15, a series of stock solution could be prepared. A given volume (200 mL) of the stock solution was poured into a stainless-steel autoclave (250 mL) and heated at 80°C for 12 h, and subsequently heated at 230°C for 24 h. The precipitated powders were separated by centrifugation, washed with deionized water and ethanol for several times, then dried in an oven at about 50°C for 30 h. For comparison, bulk YBO_3:Nd^{3+} was obtained by a direct solid-state reaction from the mixture of Y_2O_3, Nd_2O_3, and H_3BO_3 at 1100°C for 10 h in air.

The phase and crystallinity of the $Y_{1-x}BO_3$:Nd_x nanoparticles were analyzed by X-ray diffraction (XRD) (Philips XD98) using Cu$K\alpha$ radiation. Transmission electronic microscopy (TEM) images were taken on a JEM-200CX microscope operating at 160 kV. TEM samples were prepared by applying a diluted drop of the particles on a holey carbon-coated copper TEM grid. The emission spectra in the NIR were recorded on a TRIAX550 monochromator (JOBIN YVON-SPEX) equipped with a PS/TC-1 detector (ELECTRO-OPTICAL SYSTEMS INC). An 800 nm LD laser was used as excitation source. All experiments were performed at room temperature.

3. Results and discussion

Fig. 1 shows the XRD patterns of $Y_{1-x}BO_3$:Nd_x nanoparticles ($x = 0$, 0.025, 0.05, 0.075, 0.10, and 0.15). The position of diffraction peaks is in accordance with the JCPDS card (16-0277) of YBO_3 crystal, which indicated that the $Y_{1-x}BO_3$:Nd_x nanoparticles with 0–15 mol% Nd^{3+} were isostructural with the YBO_3 crystal. However, the relative intensities of different peaks of YBO_3 ($x = 0$) nanoparticles prepared by the hydrothermal method in this work were greatly different from that of JCPDS card (16-0277). The mismatch of relative intensity of XRD peaks can be attributed to the preferential nucleation and growth of YBO_3 nanoparticles along certain plane. Wang et al. [14] and Jiang et al. [15] have attributed the selectivity of the growth to the hydrothermal process and synthesis temperature, respectively. From Fig. 2, it can be found that the relative intensities of diffraction peaks (002) and (004) vs. (001), which is the strongest peak according to JCPDS card (16-0277), decreased obviously with increase in the doping concentration of Nd^{3+} ions. The relative intensities of different peaks of $Y_{0.85}BO_3$:$Nd_{0.15}$

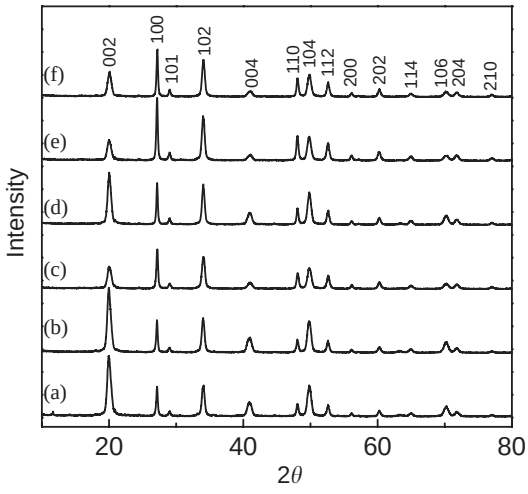

Fig. 1. XRD patterns of $Y_{1-x}BO_3$:Nd_x nanoparticles: (a) $x = 0$, (b) $x = 0.025$, (c) $x = 0.05$, (d) $x = 0.075$, (e) $x = 0.10$, and (f) $x = 0.15$.

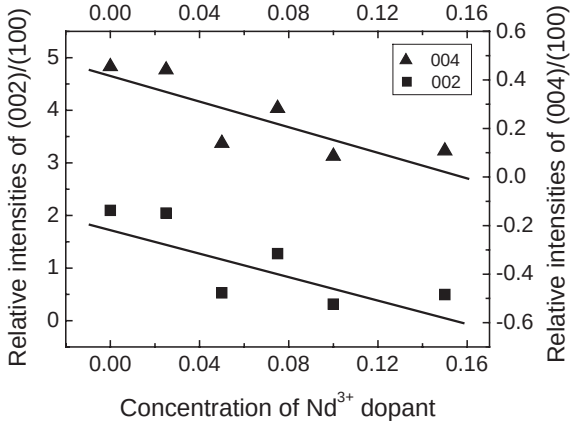

Fig. 2. Relationship between the relative intensities of diffraction peaks of (002) and (004) vs. (001) and the concentration of Nd^{3+} ion dopant.

nanoparticle can be observed to be well accordant with the JCPDS card (16-0277). Therefore, the dopants of Nd^{3+} ions weaken the selectivity of the growth of $Y_{1-x}BO_3$:Nd_x nanoparticles. From Fig. 1 it can also be found that the single phase of YBO_3 crystal can still be obtained even at a higher doping concentration (15 mol%) of Nd^{3+} ions, indicating that the Nd^{3+} ions can easily substitute the Y^{3+} sites and form a solid solution of (Y, Nd)BO_3 crystals. The solid solution is complete for $Y_{1-x}BO_3$:Nd_x with $0<x<0.15$.

Fig. 3 shows the TEM images of $Y_{1-x}BO_3$:Nd_x nanoparticles ($x = 0.025$, 0.05, and 0.10). Flake-like morphology with the size in the range 40–60 nm can be observed, which can be attributed to the preferential growth of the $Y_{1-x}BO_3$:Nd_x nanoparticles along a certain plane. The Scherrer-calculated diameter from XRD patterns is about 30 nm, which is approximately consistent with the particle component diameter observed in the TEM images. It is obvious that the aggregation of $Y_{1-x}BO_3$:Nd_x nanoparticles did not occur during the sample preparation. From Fig. 3 it can also be found that the diameter of $Y_{1-x}BO_3$:Nd_x nanoparticles became slightly smaller with increase in the concentration of Nd^{3+} dopant, which also indicated that the substitution of Y^{3+} ions by Nd^{3+} ions weakened the preferential nucleation and growth of $Y_{1-x}BO_3$:Nd_x crystals.

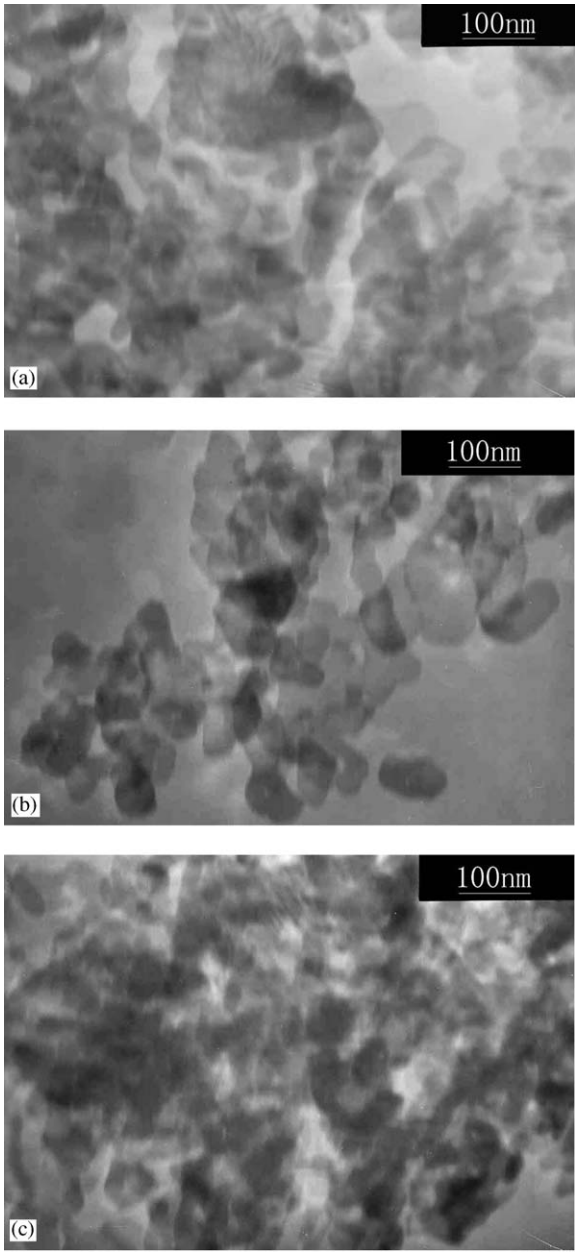

Fig. 3. TEM micrographs of $Y_{1-x}BO_3$:Nd_x nanoparticles: (a) $x = 0.025$, (b) $x = 0.05$, (c) $x = 0.10$.

Fig. 4 shows the emission spectrum in the NIR of the 10 mol% Nd^{3+}-doped nanoparticles (excited at 800 nm). The emission peaks that were observed around 1050 and 1320 nm can be attributed to the $^4F_{3/2} \rightarrow {}^4I_{11/2}$ and $^4F_{3/2} \rightarrow {}^4I_{13/2}$ transitions of Nd^{3+} ions, respectively. In comparison with the other Nd^{3+}-doped nanoparticles [6,16], the emission bands in the NIR of the Nd^{3+}-doped $Y_{1-x}BO_3$:Nd_x nanoparticles can be observed to be more narrow and sharp. Two emission peaks corresponding to the $^4F_{3/2} \rightarrow {}^4I_{11/2}$ transitions can be observed. This phenomenon could be attributed to the crystal structure of $Y_{1-x}BO_3$:Nd_x nanoparticles. Some research results on the crystal structure of YBO_3 have been reported [17–20] and now the pseudo-vaterite with space group $P6_3/m$ is widely accepted [20]. The Y^{3+} ions are eightfold coordinated by oxygen atoms in the crystal structure of YBO_3. Two types of environments for Y^{3+} ions were observed due to the delocalization of oxygen atoms [20]. The Nd^{3+} ions substitute generally the Y^{3+} sites in the $Y_{1-x}BO_3$:Nd_x crystal and thus there are two types of environments for Nd^{3+} ions. For both the sites having the C_3 symmetry, Nd^{3+} ions lying in the two sites have a similar luminescence behavior. Therefore, the emission bands of $Y_{1-x}BO_3$:Nd_x nanoparticles were not broadened and maintained the typical sharp, narrow spectra lines of Nd^{3+} ions. This kind of spectra

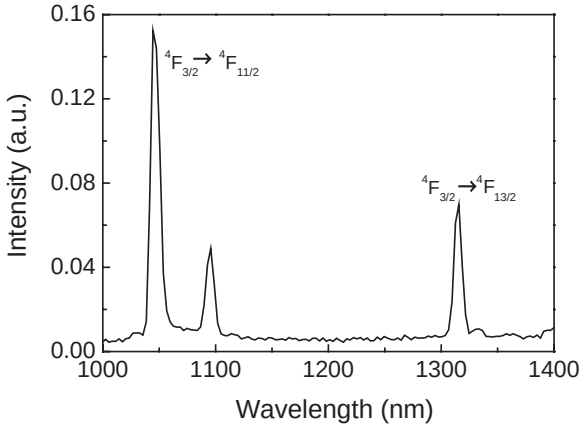

Fig. 4. Emission spectrum in the NIR of $Y_{0.9}BO_3$:$Nd_{0.1}$ nanoparticles.

characteristic makes them an ideal biological label because high resolution could be achieved when performing fluorescence assay.

Fig. 5 shows the dependence of the luminescence intensity of $Y_{1-x}BO_3:Nd_x$ nanoparticles and bulk samples on the doping concentration of Nd^{3+} ions by monitoring the emission of $^4F_{3/2} \rightarrow {}^4I_{11/2}$ transition at 1050 nm. The luminescence intensity of bulk $YBO_3:Nd^{3+}$ decreases with increasing concentration of Nd^{3+} ion dopant. For nanoparticles, the luminescence intensity increased with the increase in dopant concentration and reached a maximum at 10 mol% Nd^{3+} doping concentration. Then, the luminescence intensity decreased significantly at 15 mol% Nd^{3+} doping concentrations due to concentration quenching. It is obvious that the nanosized particles resulted in the delay in concentration quenching. The concentration quenching of the rare-earth ions-doped crystals can generally be attributed to the possible non-radiative transfer that resulted from resonance energy transfer between neighboring rare earth ions. The concentration quenching is a common loss mechanism for active laser centers. This phenomenon, however, would be expected to occur at much lower concentrations. In Nd:YAG single crystals, for example, concentrations greater than 1 wt% show a loss of signal. The concentration quenching can be suppressed by providing specific structural units in the host lattice, thereby separating the Nd^{3+} ions. Bondar et al. reported suppressed concentration quenching with a neodymium-doped pentaphosphate single crystal [21]. The phosphates may act as spacers between Nd^{3+} ions, so concentration quenching occurs at a higher concentration of Nd^{3+} ions. It is generally observed that glasses can be doped with higher levels of Nd^{3+} ions than single crystals. Koechner reported that Nd^{3+} ions doped in glass are typically used at levels of about 3 wt% [22]. The increase of dopant concentration could be due to the amorphous structure of the glass. In a crystal, the Nd^{3+} ions will be located at specific substitutional sites and will have a tendency to cluster. In the amorphous structure of glass, however, Nd^{3+} ions can undergo a more random substitution without causing much strain. Bender et al. pointed out that another mechanism of the delay in concentration quenching could be due to the nanosized particles [23]. It is speculated that Nd^{3+} ions on the surface of the nanoparticle may have luminescence properties different from those in the bulk. It is known that ions on the surface do not have a full coordination sphere, and this leads to surface atoms having a higher potential energy. As nanoparticles have a higher proportion of surface ions to bulk ions than do larger particles, more Nd^{3+} ions would reside at the surface of a nanoparticle. The incomplete coordination of the surface ions could result in more radiative decay rather than nonradiative decay of Nd^{3+} ions [23]. On the other hand, since clusters of Nd^{3+} ions and resonance energy transfer only occur within one particle due to the hindrance by the particle boundary, the clusters of Nd^{3+} ions and resonance energy transfer would decrease with decreasing diameter of $Y_{1-x}BO_3:Nd_x$ nanoparticles. Therefore, the concentration quenching generally occurs at higher dopant concentration of Nd^{3+} ions in smaller nanoparticles in comparison with the bulk sample. Thus, a desirable characteristic of $Y_{1-x}BO_3:Nd_x$ nanoparticles could be obtained by doping more Nd^{3+} ions into the host YBO_3 nanoparticles so that they were of great benefit to their practical uses.

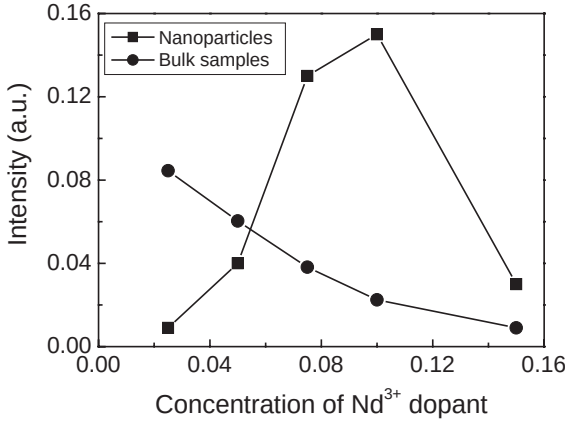

Fig. 5. Relationship between the luminescence intensity and the concentration of Nd^{3+} ion dopant for $Y_{1-x}BO_3:Nd_x$ nanoparticles and bulk samples.

4. Conclusion

Luminescent $Y_{1-x}BO_3:Nd_x$ nanoparticles were prepared by a mild hydrothermal method in the presence of urea, and a well-crystallized hexagonal phase could be obtained at low temperature. The preferential nucleation and growth of $Y_{1-x}BO_3:Nd_x$ nanoparticles along a certain plane have been observed and the dopants of Nd^{3+} ions would weaken the selectivity of the growth of $Y_{1-x}BO_3:Nd_x$ nanoparticles. The emission spectrum in the NIR of $Y_{1-x}BO_3:Nd_x$ nanoparticles consisted of a few narrow, sharp lines corresponding to the $^4F_{3/2} \rightarrow {}^4I_{11/2}$ and $^4F_{3/2} \rightarrow {}^4I_{13/2}$ transitions of Nd^{3+} ions. The luminescence intensity of $Y_{1-x}BO_3:Nd_x$ nanoparticles increased remarkably with increase in the doping concentration of Nd^{3+} ions, and reached a maximum at approximately 10 mol%. The emission bands of $Y_{1-x}BO_3:Nd_x$ nanoparticles maintained the typical sharp, narrow spectra lines of Nd^{3+} ions. This kind of spectra characteristic makes them an ideal fluorescence label in the NIR for bioassays and biosensors.

Acknowledgments

The authors gratefully acknowledge financial support for this research from the National Nature Science Foundation of China (No. 50372059, 50272059).

References

[1] T. Justel, H. Nikol, C. Ronda, Angew. Chem. Int. Ed. 37 (22) (1998) 3085–3103.
[2] B.H.T. Chai, S.A. Payne, New Materials for Advanced Solid State Lasers, MRS Symposium Series, Vol. 329, Materials Research Society, Pittsburgh, PA, 1994.
[3] D.B. Barber, C.R. Pollock, L.L. Beecroft, C.K. Ober, Opt. Lett. 22 (1997) 1247–1249.
[4] K. Kawano, K. Arai, H. Yamada, N. Hashimoto, R. Nakata, Sol. Energy Mater. Sol. Cells 48 (1997) 35–41.
[5] H. Meyssamy, K. Riwotzki, Adv. Mater. 11 (1999) 840–844.
[6] G.A. Hebbink, J.W. Stouwdam, D.N. Reinhoudt, F.C.J.M. van Veggel, Adv. Mater. 14 (16) (2002) 1147–1150.
[7] A. Huignard, V. Buissette, G. Laurent, T. Gacoin, J.-P. Biolot, Chem. Mater. 14 (2002) 2264–2269.
[8] G.S. Yi, B.Q. Sun, F.Z. Yang, D.P. Chen, Y.X. Zhou, J. Cheng, Chem. Mater. 14 (2002) 2910–2914.
[9] C.R. Ronda, J. Lumin. 72–74 (1997) 49–54.
[10] F.J. Avella, O.J. Sovers, C.S. Wiggins, J. Electrochem. Soc. 114 (1967) 613–616.
[11] M. Rem, J.H. Lin, Y. Dong, L.Q. Yang, M.Z. Su, L.P. You, Chem. Mater. 11 (6) (1999) 1576–1580.
[12] Yong Yune Shin, Jean Chae, Tae Hwan Cho, Ho Jung Chang, Sungkyoo Lim, Rhim Youl Lee, Youhyuk Kim, IDW-96, p. 81.
[13] E. Sluzky, M. Lemoine, K. Hesse, J. Electrochem. Soc. 141 (1994) 3172–3176.
[14] Y.H. Wang, K. Uheda, H. Takizawa, T. Endo, Chem. Lett. 3 (2001) 206–207.
[15] X.C. Jiang, C.H. Yan, L.D. Sun, Z.G. Wei, C.S. Liao, J. Solid State Chem. 175 (2003) 245–251.
[16] V. Buissette, A. Huignard, T. Gacoin, J.-P. Boilot, P. Aschehoug, B. Viana, Surf. Sci. 532–535 (2003) 444–449.
[17] R.E. Newnham, M.J. Redman, R.P. Santoro, J. Am. Ceram. Soc. 46 (1963) 253–256.
[18] W.F. Bradley, D.L. Graf, R.S. Roth, Acta Crystallogr. 20 (1966) 283–287.
[19] J. Hölsä, Inorgan. Chim. Acta 139 (1987) 257–259.
[20] G. Chadeyron, M. El-Ghozzi, R. Mahiou, A. Arbus, J.C. Cousseins, J. Solid State Chem. 128 (1997) 261–266.
[21] I.A. Bondar, B.I. Denker, A.I. Domanskii, T.G. Mamelov, L.P. Mezentseva, V.V. Osiko, I.A. Shcherbakov, Sov. J. Quantum Electron. 7 (1977) 167–171.
[22] W. Koechner, Solid-State Laser Engineering, Springer, New York, 1976, p. 61.
[23] C.M. Bender, J.M. Burlitch, D. Barber, C. Pollock, Chem. Mater. 12 (7) (2000) 1969–1976.